

# [O III] interferometry of the ring nebula NGC 6888

T. A. Lozinskaya, A. I. Lomovskii, V. V. Pravdikova, and V. G. Surdin

*Shternberg Astronomical Institute, Moscow*

(Submitted April 12, 1988)

*Pis'ma Astron. Zh.* **14**, 909-919 (October 1988)

Fabry-Perot interferometry with a two-stage fiber-optics image tube on the 125-, 60-cm Crimean reflectors (resolution 10"-12", 18"-24" in angle,  $\sim 15$  km/sec along the spectrum) has yielded information on the kinematics of the ring nebula NGC 6888 in the  $\lambda 5007$  [O III] line. Measurements at 80 points of the nebula show that the [O III] profile splits into three components: emission by background H II regions is flanked by that from the approaching and receding sides of the thin expanding shell. Each of the latter components has a halfwidth and peak-intensity  $V_r$ , variation of  $\lesssim 20$  km/sec, or 20% of the expansion velocity. The  $V_r$  field derived from 369 measurements in [O III] and from earlier H $\alpha$ , [N II] data permits recovery of the shell geometry and expansion rate. The model best fitting the observations is a prolate ellipsoid inclined 20°-40° to the sky, expanding on the average at  $88 \pm 12$  km/sec. No evidence is found for either oblate-ellipsoid or dumbbell geometry. The small-scale kinematics is more compatible with a wind-blown bubble than with ejection by the central star.

## 1. INTRODUCTION

The multishell hierarchical structure found in the medium around certain stellar associations is the target of an ongoing research program at the Shternberg Institute. Continuing our study of the ISM near the Cygnus OB1 association,<sup>1</sup> we here describe some new observations of the ring nebula NGC 6888 surrounding the Wolf-Rayet star HD 192163.

Among all ring nebulae around Wolf-Rayet and Of stars, NGC 6888 is the best known and most fully investigated object. The comprehensive spectroscopic, interferometric, and radio observations of this nebula may be summarized as follows (see also a recent monograph by one of us<sup>2</sup> and the references therein). Forming a 12'  $\times$  17' elliptical filamentary shell (Fig. 1a), NGC 6888 lies at a distance  $r = 1.4$ -2.3 kpc. Its central type WN 6 star, HD 192163, belongs to the Cyg OB1 association<sup>3</sup> (distance  $r = 1.8$  kpc). In the bright filaments the gas temperature  $T_e = 19,000 \pm 4000$  K, and the electron density there is  $n_e = 400$ -1500  $\text{cm}^{-3}$ . The bright optical filaments appear against a faint diffuse background. The whole system of optical filaments and condensations is expanding at an average speed of  $\sim 90$  km/sec. At radio frequencies the pattern is identical to the optical image; the radio spectrum is thermal. The total mass of ionized gas in NGC 6888 is about  $5 M_\odot$ . There is some evidence<sup>4</sup> that the chemical composition is abnormal: the heavy-element abundance may be enhanced.

Even the earliest detailed analyses of the physical environment and kinematics<sup>5,6</sup> showed that NGC 6888 fits nicely into theories for the interaction of stellar winds with the interstellar medium. Using the model of Weaver et al.,<sup>7</sup> one can demonstrate that the wind power and duration required to sweep out a shell of radius  $R \approx 4$  pc, expanding at  $\sim 100$  km/sec into a medium of density  $n_0 \approx 1$ -2  $\text{cm}^{-3}$ , are  $L_w \approx (1-2) \cdot 10^{37}$  erg/sec and  $t \approx 2 \cdot 10^4$  yr. The mass-loss parameters observed in HD 192163 are  $\dot{M} = 2.3 \cdot 10^{-5} M_\odot/\text{yr}$ ,  $V_\infty = 2000$  km/sec, corresponding to  $L_w \approx (3-4) \cdot 10^{37}$  erg/sec. During the lifetime of the nebula, the WN 6 star has lost  $\Delta M \approx 0.5 M_\odot$  of metal-enriched matter in the form of wind. Its mixing with 4-5  $M_\odot$  of wind-blown interstellar gas might account for the anomalous composition observed in NGC 6888.

Further study of ring nebulae around Wolf-Rayet and Of stars is now being widely done and has raised some new questions. In particular, it is not yet entirely clear how the two possible mechanisms for the origin of these nebulae are interrelated: detachment of an envelope, or stellar wind sweeping out the ambient gas. We lack a definite answer as to why, despite the predictions of theory, no more than half the stellar-wind sources are surrounded by ring shells. Nor is the mechanism that dissipates the wind energy in the ISM well understood. Perhaps the hot wind plasma may stream through irregularities in cool, dense, swept-up envelopes, shortening their life.<sup>8</sup> It is unclear what is responsible for the asymmetry of many ring nebulae, and NGC 6888 in particular: the patchiness of the ISM or asymmetric mass loss by the central star.

The x-ray image of NGC 6888 might, in principle, corroborate a bipolar outflow from the central star. In the 0.2-3.5 keV energy range two hot spots have been observed, fitting into diametrically opposite regions of the envelope along the major axis of the elliptical nebula.<sup>9,10</sup> It is interesting to note in this regard that the optical image, including the bright crosswise filaments at the center, could represent a three-dimensional dumbbell-type model viewed in projection.<sup>11</sup> This is one reason why it should be very instructive to recover the spatial geometry of NGC 6888 from its projected pattern and from the radial-velocity distribution of its filaments. Such analyses have been attempted on two previous occasions: from interferometry in the H $\alpha$ , [N II] lines<sup>6</sup> and from interferometric data in [N II] only.<sup>11</sup> In each case no more than 30-40 radial-velocity measurements were available.

In this letter we present the results of detailed new interferometry of the nebula in the [O III] line. These observations have had two objectives. First, we have sought to increase the number of filaments and knots with a  $V_r$  measurement, so as to warrant more trustworthy conclusions about the spatial structure of the nebula. Furthermore, comparison of photographs of NGC 6888 taken in the H $\alpha$ , [N II], [S II], and [O III] lines has revealed distinctions in morphology, perceptible even in the small-scale reproductions of Figs. 1a, b (see also the photographs published by Parker<sup>12</sup>). Perhaps

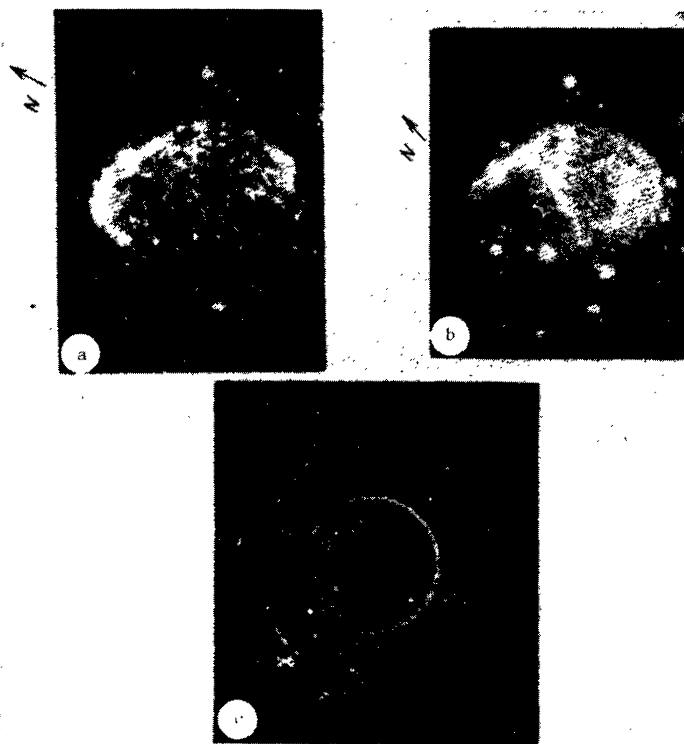


FIG. 1. The ring nebula NGC 6888. a) A photograph taken in the  $\lambda 6584$  [N II] line; b) a photograph in the  $\lambda 5007$  [O III] line; c) an [O III] interferogram, in which the outer fringe is a laboratory  $\lambda 5015.68$  He I line and the faint inner fringe represents the [O III] line, perceptibly split into several components (see Sec. 4).

regions that are radiating in lines of higher and lower ionization states differ in their internal motions.

## 2 OBSERVATIONS

NGC 6888 was observed interferometrically in the  $\lambda 5007$  [O III] line with a Fabry-Perot etalon; a focus-shortening system having a fast ( $f/1$ ) objective was mounted at the Cassegrain foci of the 125- and 60-cm reflectors at the Southern Station of the Shternberg Astronomical Institute in the Crimea. An interference filter with parameters  $\lambda_{\max} = 5006 \text{ \AA}$ ,  $\Delta\lambda_{1/2} = 14 \text{ \AA}$  provided preliminary monochromatization. The radiation detector was a two-stage fiber-optic image tube. Contact photographs were taken on Kodak 103a-G emulsion.

The Fabry-Perot mirrors had about 95% reflectivity, so that the reflection finesse was  $N_e \approx 20$ . The optimum separation of the reflecting surfaces is determined by (a) the criterion that the width of the etalon instrumental response be minimized so as to match the resolution of the image-tube screen; (b) the spectral-dispersion interval required to survey a nebula expanding at high velocity, without the wings of the lines overlapping; and (c) the need to discriminate against background emission noise. In our case the separation was  $t = 0.11 \text{ mm}$ .

The interferometer had the following operating parameters: linear dispersion in the serviceable part of the central fringe,  $\sim 5 \text{ \AA/mm}$ ; dispersion range on a radial-velocity scale,  $\sim 750 \text{ km/sec}$ ; theoretical instrumental-profile width  $\Delta\lambda \approx 10 \text{ km/sec}$ ; angular resolution corrected for the width of the actual spectral-line profile,  $18''\text{-}24''$  and  $10''\text{-}12''$  for the 60-, 125-cm reflectors, respectively.

To establish the center of the interference fringes, to convert wavelengths to a radial-velocity scale, and to construct the true instrumental profile of the interferometer, a laboratory  $\lambda 5015.68$  He I line fringe was recorded on each interferogram.

Altogether 66 interferograms each exposed 30-40 min were taken with the two telescopes, so placed that the [O III] interference fringe covered essentially the whole image of NGC 6888, including nearby regions out to  $20'\text{-}30'$  from the nebula boundary.

## 3. DATA PROCESSING

The interferograms were scanned automatically (either the whole pattern or along selected radial directions), using a Lirepho or Joyce Loebel microdensitometer. A 5-mm diameter working section of each plate was traced with a  $50 \times 50 \mu$  or  $25 \times 25 \mu$  slit, giving a  $101 \times 100$  or  $201 \times 200$  array, respectively.

Photographic densities were converted to relative intensities by standard procedure, using a characteristic-curve program developed at the Astronomical Council in Moscow.<sup>13</sup> This preliminary processing was done on a Nova 3-12 computer-controlled Joyce Loebel automated microdensitometer, with magnetic-tape readout, and the digital information was further processed on an ES 1045 computer.

To derive a spectral profile of the [O III] line from a radial scan of an interferogram, a two-dimensional linear interpolation was performed within the away of intensity values. Standard formulas converted the distances along the radius to an [O III] radial-velocity scale, using the laboratory He I reference line. This conversion utilized the equivalent focal length of the image-tube + objective system, which was ascertained from the radii of several consecutive He I interference fringes on interferograms taken with different adjustments of the etalon. In this way an empirical relation was established between the equivalent focal length and the distance from the center of the image-tube screen, allowing for the departure of the magnification from unity and for distortions in the particular image tube at the operating voltage.

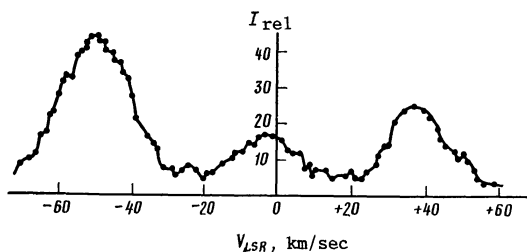


FIG. 2. A sample [O III] line profile for the central part of NGC 6888. The zero-velocity component derives from galactic background radiation; the two shifted components are emitted by the approaching and receding sides of the nebular shell. This microphotometer tracing has not been corrected for instrumental profile.

The separation between the Fabry-Perot reflecting surfaces was also measured by an empirical interferometric method, in which the fringe radii observed for about ten laboratory Ne, Kr, Hg, He lines are compared against the values computed for differing separator thicknesses. The combined error of a single  $V_r$  measurement, including the uncertainties in the equivalent focal length and in the etalon plate separation, was at most 10 km/sec.

In determining the radial velocity at the peak of the line, we did not attempt to correct rigorously for the nebula's integrated brightness distribution in the line, because two ill-posed problems would have had to be solved. A rough correction was applied for the nonuniformity of the nebular image by using monochromatic photographs taken in the [O III] line. To construct the line profile we selected only those parts of the [O III] image where the brightness varies by no more than (20-30)% along radial cross sections of the ring. As a result the error in estimating  $V_r$  at the line peak was limited to  $\sim 7$  km/sec.

The width of the [O III] line was corrected for instrumental distortions on the premise that the instrumental profile of the Fabry-Perot interferometer with its image tube, as well as the true and observed line profiles, are all Gaussian. The true instrumental-profile width, including corrections for errors in the etalon adjustment and plate surfaces, temperature instabilities, and the resolution of the light detector, was determined for each interferogram with respect to the laboratory He I line fringe; its value was at most 20 km/sec.

#### 4. RESULTS AND DISCUSSION

The interferogram of Fig. 1c strikingly demonstrates the effect of expansion by the nebular shell: although the [O III] line is narrow in the bright outlying filaments, in the central region it splits into three components, representing background emission and the approaching and receding sides of the envelope. The separation of the components corresponding to the opposite sides increases systematically from the edge toward the center because of the expansion.

As an example, Fig. 2 shows a microphotometer tracing of the [O III] line displaying the central component due to the emission of background H II regions, flanked by two shifted components emitted in the NGC 6888 shell itself.

Following the procedure of Sec. 3, we have determined the radial velocities at the peaks of individual lines or of well-resolved components of

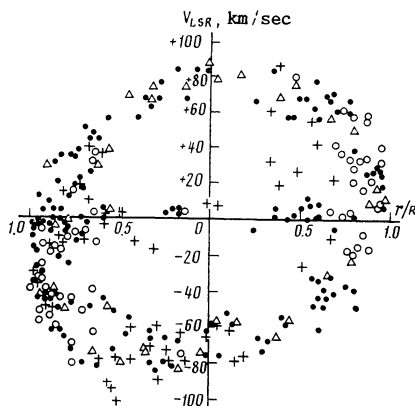


FIG. 3. Radial velocities (relative to the Local Standard of Rest) of filaments within a 4' wide strip along the NGC 6888 major axis, as a function of the normalized distance from the center. Dots, the present [O III] observations; crosses, H $\alpha$  observations by one of us<sup>6</sup>; triangles, Trefers and Chu's H $\alpha$  data<sup>14</sup>; circles, Johnson and Songathaporn's measurements in the [N II] line.<sup>11</sup>

split lines at 80 points of the nebula. On comparing the H $\alpha$ , [N II], [O III] interferometry of NGC 6888 in the present and two previous series,<sup>6,8</sup> all carried out with the same instrumentation at the focus of the 125-cm reflector, we arrive at the following conclusions.

Each of the three lines exhibits the same three emission components: the galactic background and the opposite sides of the expanding shell.

In the nitrogen line NGC 6888 exhibits a more patchy morphology than in H $\alpha$  and [O III], as is apparent from both monochromatic and interference photographs of the region. The separation between the two [O III] line components emitted by opposite sides of the expanding shell increases systematically from the edge toward the center of the nebula. The random fluctuations in the velocity at the peak of each component amount to no more than 15-20 km/sec. Such behavior of the line profile suggests that the [O III] line originates in a thin, regularly expanding envelope.

The average halfwidth of the [O III] line, combining the thermal and turbulent gas velocities in the thin shell with the width of the true instrumental profile, is  $\Delta V_{1/2} = 20 \pm 12$  km/sec. This value is based on measurements of the line width in the outlying filaments, where expansion effects are insignificant, or on the measured widths of the separate components of the split profile. Much the same value, 17 km/sec, has been obtained by Y. H. Chu (private communication) with an echelle spectrometer.

Despite certain disparities in the morphology of NGC 6888 in different lines of the optical spectrum, we have not detected any significant distinctions in the velocities of the bright-filament system as determined from the H $\alpha$ , [N II], and [O III] lines. To illustrate, Fig. 3 shows how  $V_{LSR}$  for filaments within a 4' wide strip along the nebula's major axis depends on the distance from the center, according to measurements in the H $\alpha$  line,<sup>6,14</sup> the [N II] line,<sup>11</sup> and the [O III] line (this letter). Notice that the four series of observations are all in good agreement. They all provide about the same velocity measurement accuracy.

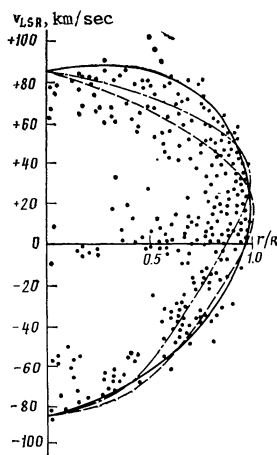


FIG. 4. Three curves computed for the radial velocity  $V_{LSR}$  as a function of the normalized distance from the center of NGC 6888. Solid curve, a prolate model ellipsoid of revolution whose major axis is inclined by  $\phi = 20^\circ$  to the plane of the sky, with the velocity vector proportional to the radius vector; dashed curve, the same model ( $\phi = 20^\circ$ ), with the velocity constant and directed radially; dot-dash curve, a model the same as the last, but with  $\phi = 40^\circ$ . The dots represent the same  $V_{LSR}$  measurements as in Fig. 3, but the points are here folded about the coordinate axes.

In our present and earlier<sup>6,8</sup> programs angular resolution was  $10''$ - $12''$  and  $18''$ - $25''$  (Sec. 2); in the other two investigations,<sup>11,14</sup> about  $1'$  and  $2'$ , respectively. We should point out that in the forbidden-line observations different methods have been utilized to calibrate against a laboratory velocity standard. We have tied our data to a He I line, determining the separator thickness by a laboratory procedure. Johnson and Songsathaporn<sup>11</sup> calibrated against interferograms of the North America Nebula, whose velocity is accurately known. Since there are no systematic differences either between these two sets of observations themselves or between them and the H  $\alpha$  measurements, which rely on a laboratory standard, we have independent evidence supporting our data processing method.

The low brightness of the filaments and the highly irregular absorption unfortunately prevent us from obtaining the  $V_{LSR}$  distribution in a strip along the minor axis of the nebula.

We have utilized the shape of the nebula in the plane of the sky and all available radial-velocity measurements (369 values of  $V_{LSR}$  at different points of the nebula from the previous<sup>6,14</sup> H  $\alpha$  and<sup>11</sup> [N II] observations and our present results for the [O III] line) to recover the true spatial geometry of the shell. The data were fitted by three configurations of expanding shells differently oriented relative to the observer: 1) an oblate ellipsoid of revolution; 2) a prolate ellipsoid; 3) the surface of revolution of a lemniscate. Model 1 could result physically from mass loss by the central star in its equatorial plane; models 2 and 3, from bipolar outflow or ejection of material. A prolate ellipsoid also might develop if the shell were expanding in a strong regular magnetic field.

Furthermore, we have considered three possible laws for the variation in expansion velocity over the surface of the shell: 1) a velocity vector proportional to the radius vector from the central star (an idealization of asymmetric mass ejection);

2) a constant velocity directed normal to the surface (an idealization of a shell expanding into a homogeneous medium due to the thermal pressure of a "hot" stellar wind); 3) a constant velocity directed along the radius vector (an idealization of a shell expanding due to the dynamic pressure of a "cool" wind).

In each case we have neglected the thickness of the shell. The Wolf-Rayet star has been regarded as the center of symmetry, and all the  $V_r$  measurements have been assumed equally accurate.

In the plane of the sky, the shape of NGC 6888 represents the projection of a prolate (oblate) ellipsoid of revolution whose axial ratio  $b/a \approx 0.7 \cos \phi$ , where  $\phi$  is the angle by which the major (minor) axis is inclined to the projection plane, or else (model 3) the projection of the surface of revolution of a lemniscate with a parameter  $a$  such that  $2\sqrt{2}a \cos \phi = b$ , where  $b$  is the diameter of NGC 6888 along its major axis.

The three-dimensional model parameters were determined by minimizing the sums of the squared deviations for the 369  $V_r$  measurements, using the Newton-Gauss method. The best fit to the observations was obtained for a prolate ellipsoidal shell. One can approximate the data equally well by using ellipsoids whose major axis is inclined to the plane of the sky by angles from  $\phi = 20^\circ \pm 10^\circ$  to  $\phi = 40^\circ \pm 10^\circ$  if the expansion velocity is constant ( $V \approx 88 \pm 12$  km/sec), or alternatively, if the velocity is proportional to the shell radius, by ellipsoids whose major axis is inclined by  $\phi = 20^\circ \pm 10^\circ$ . The corresponding axial ratios of the ellipsoids of revolution range from  $b/a = 0.66$  to  $0.54$ .

As an illustration, Fig. 4 shows the observed filament radial velocities  $V_{LSR}$  (dots) compared with theoretical curves expressing the dependence of  $V_{LSR}$  on the normalized distance from the center (only in a  $4'$  wide strip along the major axis) for each of three prolate-ellipsoid models.

The large spread in radial velocities, owing both to measurement errors and to real velocity fluctuations, as well as the low accuracy with which some measurements can be localized relative to the projected image of the nebula, preclude further refinement of the model. It is impracticable, for example, to ascertain how the velocity varies over the surface of the shell, to allow for an eccentric placement of the Wolf-Rayet star, or to accommodate departures of the nebula's shape from our idealized configuration.

## 5. SUMMARIZING REMARKS

The observations described above represent the first comprehensive analysis of the kinematics of NGC 6888 in the [O III] line. The morphological differences in the H  $\alpha$ , [N II], [S II], [O III] lines identifiable on monochromatic photographs of the nebula (and Parker's photographs<sup>12</sup>) suggest possible disparities in the internal velocities of gas radiating in lines of different ionization states. However, the H  $\alpha$ , [N II], [O, III] line measurements show no substantial differences in the large-scale kinematics of the shell.

From the [O III] data the shell appears to be thin, and the internal-velocity dispersion in the thin shell is decidedly smaller than the systemic expansion velocity. Compared with an average expansion rate of 90 km/sec, the random velocities of

filaments on the same side of the shell differ by 15-20 km/sec at most. The [O III] line halfwidth due to thermal and turbulent motions in the envelope is  $\Delta V_{1/2} = 20 \pm 12$  km/sec.

Our [O III] interferometry has been combined with previous H $\alpha$  and [N II] data<sup>6,14,11</sup> (369 measurements of  $V_p$ , covering almost the whole field of the nebula) to permit recovery of the shell's spatial geometry and expansion-velocity law. Three models have been tested to fit this geometry; prolate and oblate ellipsoids of revolution and a lemniscate surface of revolution; at each point of the shell the velocity has been assumed constant (directed normal to the surface or radially), or proportional to the shell radius. These choices encompass a variety of possibilities for the nature of the nebula, including a shell thrown off by the star or swept out by stellar wind; in the latter case the shell could expand through either thermal pressure of a hot wind or dynamic pressure of a cool wind.

The best fit to the observations is obtained for a prolate ellipsoid of revolution whose major axis is tilted by  $\phi = 20^\circ$ - $40^\circ$  to the sky (true axial ratio  $b/a = 0.54$ - $0.66$ ) and which is expanding at  $88 \pm 12$  km/sec. A shell of this shape could result from asymmetric (bipolar) mass loss by the central star or from expansion into a medium with a strong, regular magnetic field. The speculations as to a possible dumbbell structure (a lemniscate surface of revolution) or even a "triple cavity"<sup>11</sup> are not supported, at least to the accuracy of the available data. The apparent double structure found<sup>9,10</sup> in the x-ray image of NGC 6888 might result either from asymmetric mass loss by HD 192163 or from absorption in a dense local cloud with which the expanding shell is colliding.<sup>11</sup> Possible evidence for such a collision is the brightening of the filaments in the central and NW parts of the nebula.

The velocity ellipse of Fig. 4 shows a distinctive asymmetry, tending to favor the model of constant expansion velocity at each point of the ellipsoid, corresponding to the shell being blown by stellar-wind pressure. But the scatter of points is too

large to rule out with any confidence a model in which the velocity is proportional to the shell radius, corresponding to ejection of matter by the central star.

A choice between these two alternatives might be made by considering the relationship deduced from the H $\alpha$  and [N II] data<sup>6,8</sup>: the velocities of the bright compact filaments and condensations were found to be substantially lower than those of the faint diffuse structures and the interfilament medium. Such behavior is quite typical for a shell that is driven by a shock wave triggered by stellar wind, and is often encountered in old supernova remnants. If on the contrary the shell has been ejected by the star, the dense knots ought to suffer less deceleration in the interstellar medium than would the diffuse interfilament gas.

- <sup>1</sup> T. A. Lozinskaya and T. G. Sitnik, *Pis'ma Astron. Zh.* **14**, 240 (1988) [*Sov. Astron. Lett.* **14**, 100 (1988)].
- <sup>2</sup> T. A. Lozinskaya, *Supernovae and Stellar Winds: Interactions with the Galactic Gas* [in Russian], Nauka, Moscow (1986).
- <sup>3</sup> R. M. Humphreys, *Astrophys. J. Suppl. Ser.* **38**, 309 (1978).
- <sup>4</sup> K. B. Kwitter, *Astrophys. J.* **245**, 154 (1981).
- <sup>5</sup> H. M. Johnson and D. E. Hogg, *Astrophys. J.* **142**, 1033 (1965).
- <sup>6</sup> T. A. Lozinskaya, *Astron. Zh.* **47**, 122 (1970) [*Sov. Astron.* **14**, 98 (1970)].
- <sup>7</sup> R. Weaver, R. McCray, J. Castor, P. Shapiro, and R. Moore, *Astrophys. J.* **218**, 377 (1977).
- <sup>8</sup> T. A. Lozinskaya, *Pis'ma Astron. Zh.* **9**, 469 (1983) [*Sov. Astron. Lett.* **9**, 247 (1984)].
- <sup>9</sup> N. G. Bochkarev, V. V. Pravdikova, T. G. Sitnik, and N. N. Piskunov, report to Soviet Natl. Conf. Wolf-Rayet Stars and Kindred Objects, Tartu (1986).
- <sup>10</sup> N. G. Bochkarev, *Nature* **332**, 518 (1988).
- <sup>11</sup> P. G. Johnson and R. Songsathaporn, *Mon. Not. R. Astron. Soc.* **195**, 51 (1981).
- <sup>12</sup> R. A. R. Parker, *Astrophys. J.* **224**, 873 (1978).
- <sup>13</sup> N. E. Piskunov, D. A. Ptitsyn, T. A. Ryabchikova, and V. L. Khokhlova, *Nauch. Inform. Astron. Soveta Akad. Nauk SSSR No.* **54**, 45 (1983).
- <sup>14</sup> R. R. Treffers and Y.-H. Chu, *Astrophys. J.* **254**, 569 (1982).

Translated by R. B. Rodman